

# A FINITE ELEMENT MODEL FOR A SELECTIVE LASER SINTERING OF A POLYCARBONATE POWDER BLOCK

Alva Edy Tontowi \*)

## ABSTRACT

A two dimensional finite element model was applied to determine temperature distribution within the layer block in the Selective Laser Sintering (SLS) of polycarbonate powders. Temperature time history and the sintering densification within the powder bed have been assumed to follow the solution of the heat conduction and the Nelson model (1993), respectively. The conductivity and the specific heat of the particle bed are treated as a function of temperature. In this model, shrinkage which usually occurred after cooling is not considered. The results show that densification depends on the temperature distribution within the powder block and the laser power or the Andrew number.

Keywords : Rapid Prototyping, Sintering, Thermal Modelling.

## INTRODUCTION

Rapid Prototyping (RP) by layer manufacturing or solid free form fabrication, first reviewed by Kruth in 1991, has continued to find new application, from concept to functional prototype, and now for prototype tooling (Berzin *et al*, 1996). Commercially machine, such as Stereolithography and Selective Laser Sintering (SLS) are among the populer machine in RP. However, in terms of the accuracy, these techniques are not as accurate as machining or moulding (Childs and Juster, 1994).

In the SLS machine as shown in Figure 1, the whole bed is heated to near the glass transition temperature. Material such as polycarbonate, this temperature is set at 154 °C. The laser supplies only the energy needed to increase the temperature into the sintering range. A common layer thickness is 0.125 mm.

During heating by the laser beam, a bed of polycarbonate powder undergoes a temperature rise and a densification. A finite element model, especially on thermal model has been considerable introduced by Nelson (1993), Weissman and Hsu (1996), Dalgarno *et al* (1996), and Childs (1997). The first and second authors developed one dimensional finite element model, while the third and the forth authors developed two dimensional model for predicting curling by employing ABAQUS software, and densification for multilayers by applying a three angular element type, respectively. In this work, the

calculation subroutine is similar to the Childs model, but a rectangular element type is used without considering shrinkage. A successful model would be at a minimum density or void fraction and temperature as a function of time and position in the sintering powder bed. Inputs for the model includes laser power, scanning speed, scan spacing, thermal properties of the material, the initial temperature of the powders, and other thermal boundary conditions.

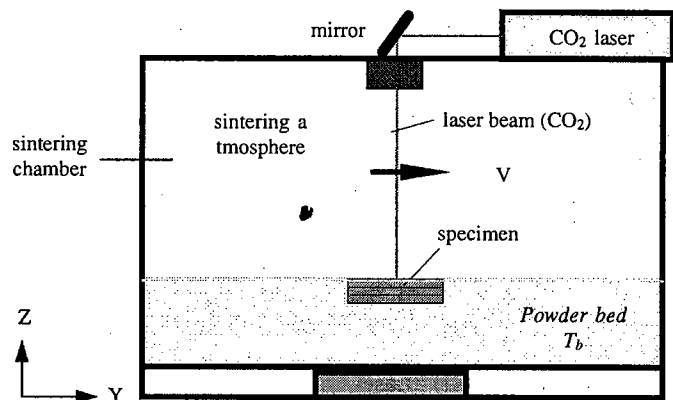


Figure 1. A physical model of a selective laser sintering process.

The problem of the modelling for the sintering of a bed of particles on microscopic scale (i.e. smaller than the particles themselves) is a computational daunting task. If the particle bed is assumed

\*) Ir. Alva Edy Tontowi, MSc., Lecturer at The Department of Mechanical Engineering UGM.

conceptually as a continuum with effective thermal properties that may depend on temperature and porosity, the task is made more tractable. The approach used by Weissman and Hsu : conductivity and specific heat of homogenized particle bed were on the based of Yagi-Kunii relationship and the solid particles because of the small of air. In this work, these properties are used as function of temperature following Nelson model (1993) i.e. the properties change by increasing temperature, and the temperature distribution is not homogen everywhere within the powder bed. The thermal conductivity is given by

$$K_s = 0.0251 + 0.0005T \quad 1)$$

and the powder bed conductivity is expressed as

$$K = K_s \frac{\rho}{\rho_s} \quad 2)$$

while, the specific heat is defined as

$$Cp_s = 935 + 2.28T \quad 3)$$

These approaches to a sintering model were used by Nelson (1993) and Ryder *et al* (1996). They used a finite difference algorithm to follow the sintering process in time and space in a single layer of powder. In this work, the first step which is presented here, demonstrates the successful application of this technique to the same problem solved by Nelson and Ryder. To carry out the finite element analysis, a computer code AET2D has been developed by the author on the based of Huebner and Thornton (1995), and the experimental condition is summarized on the Table 1.

Table 1. Experimental Condition

Laser power $P$ (watt) ; Laser type	6, 11, 22 / CO <sub>2</sub> (CW)
Scanning speed $U$ (mm/s)	860
Scanning space $s$ (mm)	0.203
Material (Amorphous)	Polycarbonate powder
Arrhenius constant (s <sup>-1</sup> )	$8.84 \times 10^{16}$
Activation energy (K)	21000
Powder density (kg/m <sup>3</sup> )	485
Solid density (kg/m <sup>3</sup> )	1200

### PHYSICAL MODEL OF POWDER BLOCK

A physical model is a single layer block of packed powder made by heating the powder bed using

a laser beam which moves from the left to the right side with speed  $V$ . The model is 25 mm wide ( $w$ ), 1.2 mm long ( $L$ ) and 0.125 mm thick ( $\Delta z$ ). The laser heat flux  $q_s$  is assumed to be a blade shape with  $d$  wide and  $w$  long and it moves along the  $y$ -direction with speed  $V$  over the powder bed. Figure 2 shows a single layer of powder block.

In the calculation scheme, the heat source is assumed to be similar within the  $x$ -direction. Therefore, thermal heat transfer along the  $y$  and  $z$ -direction or inside the block, can be represented by using 2-dimension model in  $y$ - $z$  coordinate axes. The results have been validated to the Childs' model.

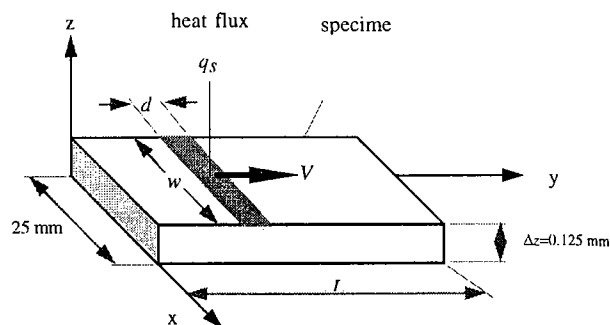


Figure 2. Domain (or specimen)

### THERMAL MODEL

A two dimensional form of the conduction heat transfer was used which represented of the physical problem of a moving heat source, scanning over the polycarbonate powder bed. The governing equation is given by

$$\rho C_p \frac{\partial T}{\partial t} = k \left( \frac{\partial q_y}{\partial y} + \frac{\partial q_z}{\partial z} \right) \quad 4)$$

The domain and boundary conditions are set as shown in Figure 3. The left ( $S_2$ ), the right ( $S_3$ ) and the bottom sides ( $S_4$ ) are defined as an adiabatic condition, and it is set at 154 °C. While on the surface, the heat source  $q_s$  is set moving from the left to the right with the velocity  $V$ . The heat flux is expressed as a relation of the laser power and it is given by

$$q_s = \frac{P}{wd} \quad 5)$$

The initial and the boundary condition were applied for the problem are as follows.

For  $t \leq 0$ ,  $T(y,z) = 154^\circ\text{C}$ ,

For  $t > 0$ , over the boundaries :

1.  $S_1 : z = Z_{bnd} ; -K \frac{dT(y,z)}{dz} = q_s$
2.  $S_2 : z = Z_{bnd} ; -K \frac{dT(y,z)}{dz} = q_s = 0$
3.  $S_2^* : z = Z_{bnd} ; -K \frac{dT(y,z)}{dz} = h(T - T_\infty)$
4.  $S_3 : -K \frac{dT(y,z)}{dy} = q$
5.  $S_4 : y = Y_{bnd}, T(y,z) = 154^\circ\text{C}$
6.  $S_5 : z = 0, T(y,z) = 154^\circ\text{C}$

The governing equation is derived from the heat conduction equation (4). By applying the weighted residual method or the Galerkin method and introducing  $\theta$ -method, this equation is written as

$$\left[ \frac{1}{\Delta t} [C] + \theta [K] \right] \{T\}_{n+1} = \left[ \frac{1}{\Delta t} [C] - (1-\theta) [K] \right] \{T\}_n + (1-\theta) \{R\}_n + \theta \{R\}_{n+1} \quad (8)$$

where,  $[C]$  is the element capacitance matrix,  $[K]$  is the element conductance matrix, and  $\{R\}_n$  is the load vector, parameter  $\theta$  can vary from 0 to 1.  $\theta = 0$  (forward difference scheme),  $\theta = 2/3$  (the Galerkin scheme and it is the favourable value),  $\theta = 0.75$  (the Tseng *et al* scheme, 1992),  $\theta = 0.878$  (the Lambert

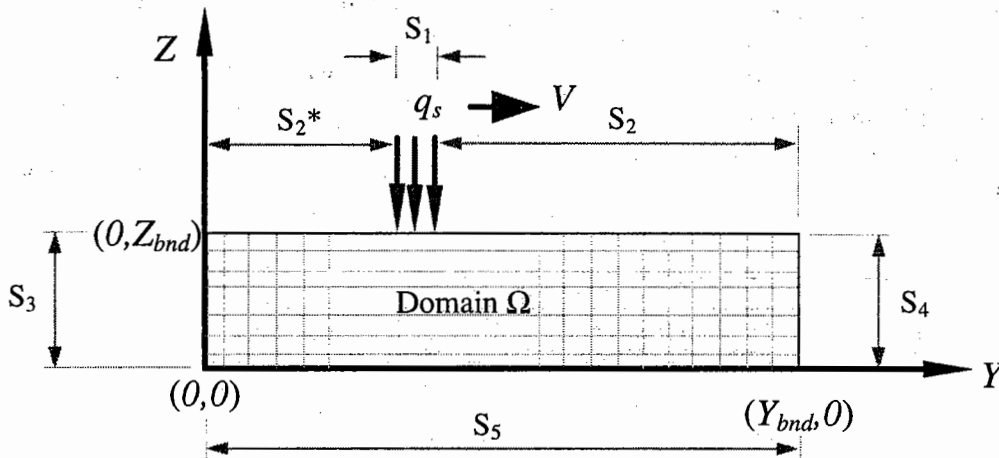


Figure 3. Domain and boundary condition.

The sintering densification is assumed to follow the Nelson model (1993), and it is given by

$$\frac{d\rho}{dt} = (\rho_s - \rho) A e^{\left( \frac{-E}{RT} \right)} \quad (6)$$

Where  $A$  is the Arrhenius constant  $= 8.84 \times 10^{16} \text{ s}^{-1}$  and  $E/R$  is activation energy  $= 21000 \text{ K}$ .

### FINITE ELEMENT FORMULATION

As formulation procedure of finite element found in the most of finite element standard book (Huebner and Thornton, 1982), the region of interest or domain  $r$  in the powder bed is subdivided into elements, and the temperature  $T$  within the element is interpolated from the nodal value  $T_i$  of the element through the interpolation function  $N_i$ .

$$T = \sum_{i=1}^r N_i T_i \quad (7)$$

scheme), and  $\theta = 1$  (the backward difference scheme). In this work  $\theta$  was taken 0.5.

In the sintering process, element load vectors  $\{R\}_n$  is equal to  $\{R\}_{n+1}$  due to at any time the value of the laser heat flux is assumed to be constant. This vector only consists of an external heat source (or a laser heat flux :  $q$ ). Hence, equation (9) becomes

$$\left[ \frac{1}{\Delta t} [C] + \theta [K] \right] \{T\}_{n+1} = \left[ \frac{1}{\Delta t} [C] - (1-\theta) [K] \right] \{T\}_n + \{R\}_n \quad (9)$$

The system of matrices  $[C]$  and  $[K]$  are obtained from the summation of all element matrices  $[C^e]$  and  $[K^e]$  in the mesh as

$$[C] = \sum [C^e] \quad (10)$$

$$[K] = \sum [K^e] \quad (11)$$

The element matrices  $[C^e]$  and  $[K^e]$  can be evaluated from the following volume integrals over the element's volume :

$$[C^e] = \int_V N^T \rho C_p N dV$$

$$[K^e] = \int_V B^T K B dV$$

12)

### MODELLING RESULTS AND DISCUSSION

The numerical results i.e. a density distribution within a single layer block (or domain) of polycarbonate, were obtained on the basis of temperature distribution which was calculated by using the 2D finite element method. Laser power were 6, 11 and 22 W or the *Andrew number*,  $P/Us$  of 0.034, 0.062 and 0.113 J/mm<sup>2</sup> (where  $U = 860$  mm/s and  $s = 0.203$  mm) have been used. Also, the density distribution for  $P/Us$  of 0.062 J/mm<sup>2</sup> is given for up to three time step positions to show the moving heat source over the powder bed.

Figure 4.1 to 4.6 show the density contours which are plotted as a function of position in the y-z coordinates. The y-direction shows the length of the powder block over which the laser beam moves to the right, while the z-direction shows the depth to which densification can be achieved for the laser power of 6, 11 and 22 W. Figures 4.1 to 4.3 show predicted densification of a single layer for one time step, while Figure 4.4, 4.5 and 4.6 show predicted densification of a single layer for  $P/Us$  of 0.062 J/mm<sup>2</sup> after, one, two and three time moving steps, respectively.

In general, the higher the laser power, the deeper and the longer, the solid part can be achieved. The strong influence of  $P/Us$  on *bonus Z* (i.e. geometric excess in z-direction) is clear. It shows how densification extends further outside the laser start position for the larger is  $P/Us$ . For  $P/Us$  of 0.034 J/mm<sup>2</sup>, the region with density 1200 kg/m<sup>3</sup> is only 0.02 mm deep and less than 0.14 mm long. Whereas, for  $P/Us$  of 0.062 J/mm<sup>2</sup> was 0.03 mm deep and 0.28 mm long, and for  $P/Us$  of 0.113 J/mm<sup>2</sup>, it was 0.04 mm deep and 0.44 mm long.

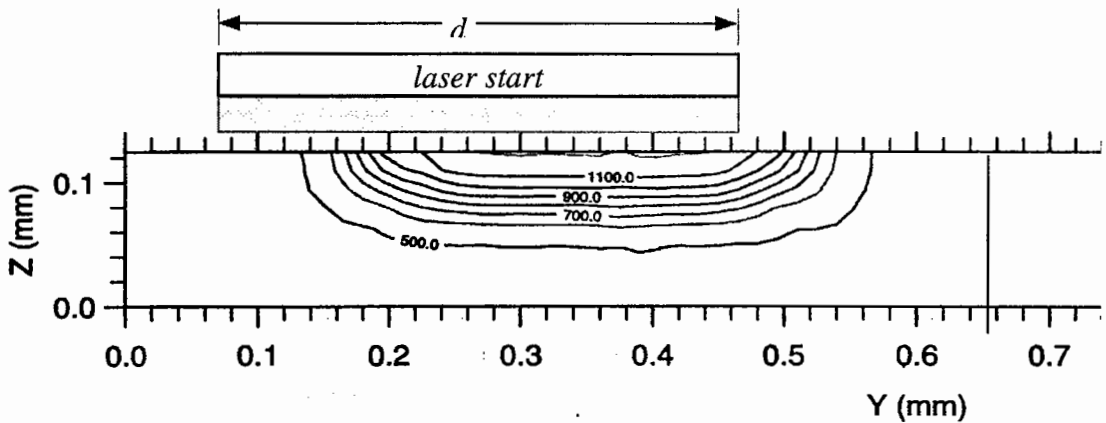


Figure 4.1. Predicted single layer densification for  $P/Us$  of 0.034 J/mm<sup>2</sup> and a single time step

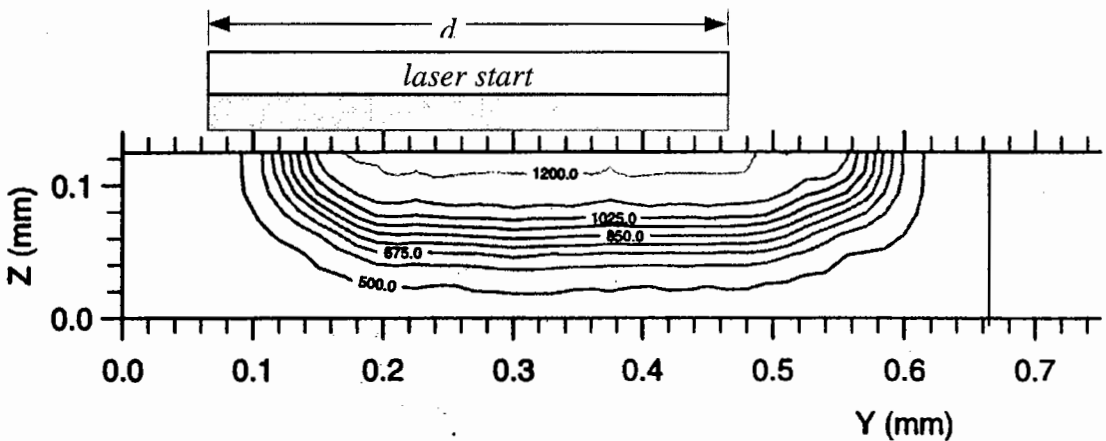


Figure 4.2. Predicted single layer densification for  $P/Us$  of 0.062 J/mm<sup>2</sup> and a single time step

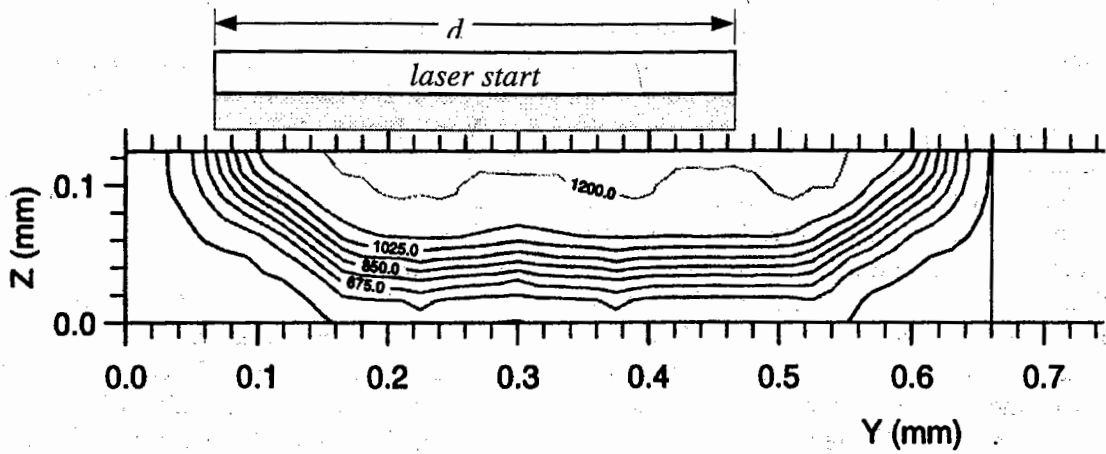


Figure 4.3. Predicted single layer densification for P/Us of  $0.113 \text{ J/mm}^2$  and a single time step

The beam movement, however, as shown in Figure 4.4, 4.5 and 4.6 did not cause a significant change on the part density. It only caused the

extension of the densified region in the direction of laser movement.

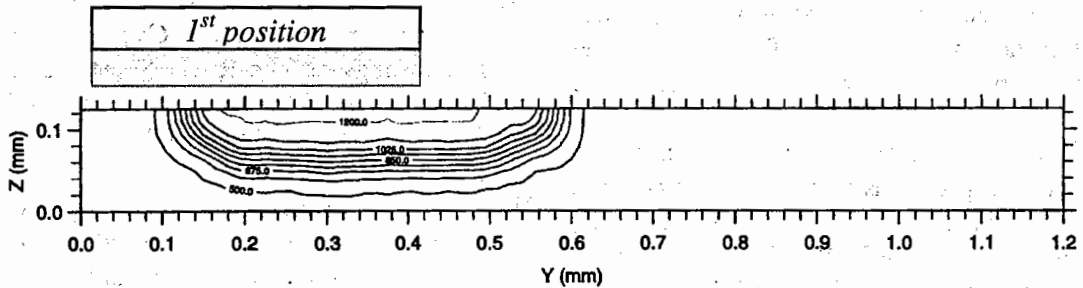


Figure 4.4. Predicted single layer densification for P/Us of  $0.062 \text{ J/mm}^2$  at the first position of the laser beam

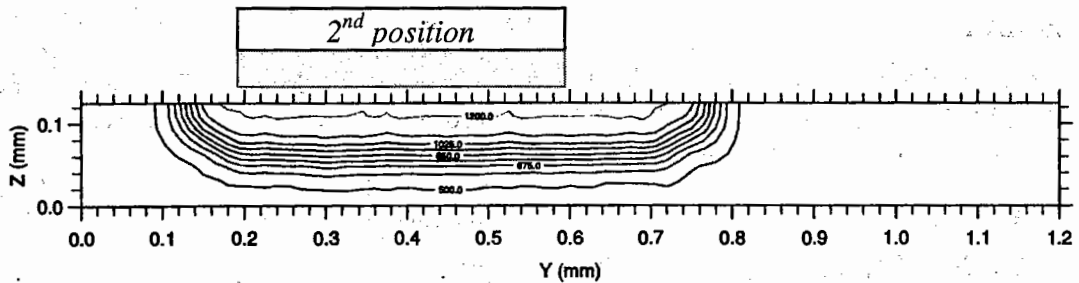


Figure 4.5. Predicted single layer densification P/Us of  $0.062 \text{ J/mm}^2$  at the second position of the laser beam

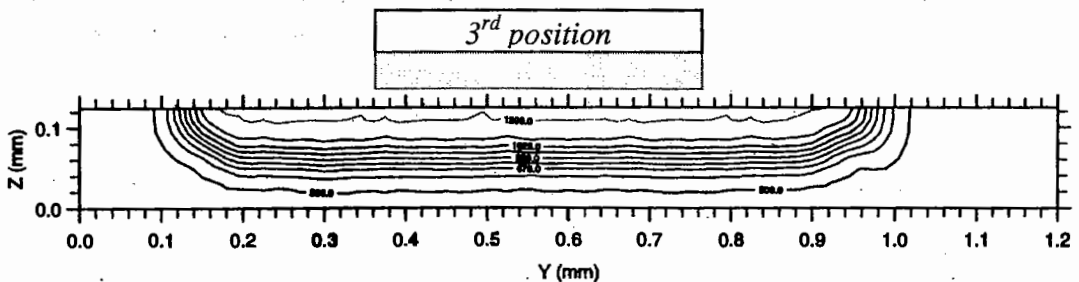


Figure 4.6. Predicted single layer densification P/Us of  $0.062 \text{ J/mm}^2$  at the third position of the laser beam

The density gradient within a single layer block mainly depends upon the temperature distribution with position (in y-z co-ordinates). The temperature distribution depends on the heat flux of the laser beam and its position on the powder bed surface along the y-axis. During sintering, the more power there is, the deeper and longer will be the solid part. As shown in Figure 4.1 to 4.3, for the same laser beam diameter (0.4 mm), there are different sizes of the solid part in y and z-direction. For example, the single layer block that was heated with the laser power of 22 W shows a different size, 0.01 mm deeper and 0.16 mm longer, than that with the laser power of 11 W. This also shows clearly of the *bonus Z* effect.

## CONCLUSION

Considering the results and discussion in the section above, it can be concluded that, the density of the single layer block depends on the temperature distribution, the position of the laser heat flux over the powder bed surface, and the position of powder particle within the y-z co-ordinate. The higher of the laser power will be the deeper and the longer of the solid part.

Several issues, such as shrinkage, curling, and defects are difficult problems that can not be covered by the current computer code at the present study. The current computer code, AET2D, is only able to estimate temperature and density distribution within the single layer specimen with 0.125 mm thick.

## ACKNOWLEDGEMENTS

The author would like to thank to Dr. M. Shiomi (Osaka University) for his suggestion in this research and Prof. T.H.C. Childs for his supervision.

## BIBLIOGRAPHY

- Berzin, M., Childs, T.H.C., Dalgarno, K.W., Ryder, G.W. and Stein G., *Densification and Distortion in Selective Laser Sintering of Polycarbonate*, Solid Freeform Fabrication Proceedings, University of Texas at Austin, 1995, 196-203.
- Carslaw, H.S. and Jaeger, J.C., *Conduction of Heat in Solids*, 2nd Edition, Oxford University Press, New York, 1959, 1-497.
- Childs, T.H.C., *Program SINTFEAM : Outline Description*, Version 1, University of Leeds, 1997.
- Childs, T.H.C., Cardie, S. and Brown, J.M., *Selective Laser Sintering of Polycarbonate at Varying Powers, Scan Speeds and Scan Spacings*, Solid Freeform Fabrication Proceedings, University of Texas at Austin, 1994, 356-363.
- Dalgarno, K., Childs, T.H.C., Rowntree, I., Rothwell, L., *Finite Element Analysis of Curl Development*, Solid Freeform Fabrication Proceedings, University of Texas at Austin, 1996.
- Huebner, K.H. and Thornton, E.A., *The Finite Element Method for Engineers*, John Wiley and Sons, Inc., 3th Ed., 1995.
- Jaeger, J.C., *Moving Sources of Heat and The Temperature at Sliding Contacts*, Journal and Proceedings of The Royal Society of New south Wales, Vol. 76, Part III, Published by The Society-Science House Gloucester and Essex Streets, 1943, 203-224.
- Nelson, J.C., *Selective Laser Sintering : A Definition of the Process and An Empirical Sintering Model*, Ph.D.- Dissertation, University of Texas at Austin, UMI-Dissertation Services, Michigan, 1993, 6-210.
- Ryder, G., Berzin, M. and Childs, T.H.C, *Modelling Simple Feature Creation in Selective Laser Sintering*, Solid Freeform Fabrication Proceedings, University of Texas at Austin, 1996, 567-574.
- Tszeng, T.C., Im, Y.T., and Kobayashi, S., *International Journal of Machine Tools Manufacturing*, 1989, 29-1, 107-120.
- Weissman, E.M. and Hsu, M.B., *A Finite Element Model of Multi-Layered Laser Sintering Parts*, Solid Freeform Fabrication Proceedings, University of Texas at Austin, 1991, pp. 86-93.